
A COMPARATIVE STUDY OF NETWORK TRAFFIC REPRESENTATIONS FOR NOVELTY DETECTION

Kun Yang

Columbia University

Samory Kpotufe

Columbia University

Nick Feamster

University of Chicago

ABSTRACT

Data representation plays a critical role in the performance of novelty detection methods from machine learning (ML). Network traffic has conventionally posed many challenges to conventional anomaly detection, due to the inherent diversity of network traffic. Even within a single network, the most fundamental characteristics can change; this variability is fundamental to network traffic but especially true in the Internet of Things (IoT), where the network hosts a wide array of devices, each of which behaves differently, exhibiting high variance in both operational modalities and network activity patterns. Although there are established ways to study the effects of data representation in supervised learning, the problem is particularly challenging and understudied in the unsupervised learning context, where there is no standard way to evaluate the effect of selected features and representations at training time. This work explores different data representations for novelty detection in the Internet of Things, studying the effect of different representations of network traffic flows on the performance of a wide range of machine learning algorithms for novelty detection for problems arising in IoT, including malware detection, the detection of rogue devices, and the detection of cyberphysical anomalies. We find that no single representation works best (in terms of area under the curve) across devices or ML methods, yet the following features consistently improve the performance of novelty detection algorithms: (1) traffic sizes, (i.e., packet sizes rather than number of packets in volume-based representations); and (2) packet header fields (i.e., TTL, TCP flags).

Keywords Outlier detection · Gaussian mixture model (GMM) · One-class support vector machine (OCSVM) · Kernel density estimation (KDE) · Autoencoder (AE)

1 Introduction

An increasing number of interconnected “Internet-of-Things” (IoT) are being deployed to monitor and manage homes, buildings, infrastructure, and even outdoor spaces. An intention of many such deployments is to monitor the environment for new, unusual, or anomalous activities—in other words, patterns that have previously not been observed. Such new or unusual activities can be indicative of many types of noteworthy events, including network or physical security incidents, device or infrastructure malfunctions, even behavioral changes in the users of the devices that might be indicative of abnormal human conditions or behaviors. The general goal of detecting such new, unseen events falls under the general category of *novelty detection* problems in machine learning, for which there are a wide variety of possible procedures, including Gaussian mixture models (GMM), one-class support vector machines (OCSVM), kernel density estimation (KDE), and others. The success of any of these procedures—and, in fact, for *any* machine learning approach—depends fundamentally on how the data are represented as input features to the model. Often the choice of features and how they are represented are more fundamental to the effectiveness of the approach than the model itself.

IoT devices provide useful “digital exhaust” that can be used to detect a broad class of new, unseen events and anomalies. Specifically, Internet-connected devices must necessarily generate network traffic as they communicate with other devices on the network (e.g., other devices on the home network, cloud-hosted services that control these devices). Unusual activities or incidents may be reflected in changes to the underlying traffic itself. As a simple example, an Internet-connected light switch generates associated traffic when it is turned on and off, effectively generating a timeseries of network traffic over time. The data itself is timestamped, and multi-dimensional—for example, the

device may talk to more than one destination on the network; the timestamped nature of the dataset makes the data itself irregularly sampled in the time domain. Intuitively, one could assume that the things that a human (or computer program) does to interact with such a device might follow some normal patterns, and that novelty detection might be interested in identifying deviations in these patterns, where those deviations might reflect anything from a malware infection to someone entering the room at an unusual or unexpected time. As Internet-connected devices become increasingly ubiquitous, the digital exhaust that these devices produce provides a wealth of signal for detecting a wide variety of anomalies for just about any activity in our daily lives. Approaches to capture novelty in the traffic that these devices generate are less well explored.

Unfortunately, representations of network traffic that are most effective for novelty detection remain a priori unclear. By default, representation choices involve various statistics on traffic volumes, decisions on packet sampling rates, and choices of observation intervals; however, which of these choices retain predictive information remains a priori unclear, especially given the large variety of IoT devices with vastly different traffic patterns. For instance, if we decide to record and build on *number of packets per second*, then changes in traffic patterns at the micro-second level might go undetected; on the other hand, recording at the microsecond level would result in higher dimensional observations that machine learning procedures might fail to scale up to, due to well-known challenges with high dimensional data¹.

Our goal is to explore how different data representations for network traffic affect novelty detection rates, across a range of IoT devices, types of novelty, and unsupervised machine learning models. Given raw traffic inputs, we focus on the problem of identifying novel network *flows*—sequences of packets from a fixed source to a fixed destination, a common, intuitive unit of identification in network traffic that, at a high-level, represents a single exchange of data between two network endpoints. From a practical perspective, the ability to identify a novel flow of course lends itself to detecting other types of novelty; for example, a device that generates novel traffic flows may itself be considered novel. There are many possible ways to represent raw traffic traces (i.e., packets) as inputs. The data itself can be aggregated on various time windows, elided, transformed into different bases, sampled, and so forth.

Results and contributions. We compare flow-based data representations as combined with various machine learning procedures for novelty detection. To compare the performance of different machine learning procedures, we report the area under the ROC curve (AUC) for each approach and each dataset. Because machine learning procedures are very sensitive to hyperparameter choices (e.g., bandwidth choice in OCSVMs, or the number of dimensions in PCA), we consider both the best possible choices of such hyperparameters, which unfortunately are hard to find in practice without labeled data, and default choices that might be made in practice based on rule-of-thumbs. To ensure an apples-to-apples comparison across procedures, we ensure that all data representations result in feature vectors of a similar order in dimension, in the range of 10 to 30 dimensions. Our primary results are as follows:

- No single data representation works best across all devices and models.
- Performing a Fourier transform on the raw network packet traces generally has minimal effect on model accuracy, regardless of the representation of the data in the time domain.
- Incorporating packet size and TCP transport header information (e.g., IP TTL, TCP flags) into the timeseries can significantly improve the accuracy of novelty detection, across a variety of models and outlier detection techniques.

Outline Section 2 outlines the common ways of representing network traffic flows in the literature. It is difficult to be completely exhaustive, yet we focus on the most established approaches for representing traffic data both in general network anomaly detection and in the growing literature on novelty detection for IoT, comparing tuning and configuration and tuning decisions that might be made in practice. Section 3 outlines the machine learning models and performance metrics that we use for our comparative analysis, as well as the metrics that we use to evaluate these models. Section 4 describes the setup of our experiments, including how we selected hyperparameters for various novelty detection models, as well as the datasets that we used in our evaluation and how we processed those datasets. Section 5 describes the results from our experiments, and Section 6 concludes with a summary and directions for future work.

2 Data Representation

The importance of data representation has in fact fostered many subfields such as *metric learning*, *representation learning* which aim to *automatically* find the right representation to be coupled with given procedures, so far with

¹The so-called *curse of dimensionality* in machine learning is the observed fact that the higher the dimension of the input, the harder it is to achieve good accuracy; in particular, we might then require an amount of training data exponential as a function of dimension.

mixed results, but with much success in application areas such as computer vision and speech processing [1]. No such automatic approach has yet been developed in the fledgling application area of novelty detection for IoT, and a main aim of this work is to bring attention to the importance of data representation, and identify representations that work well in general while meeting practical needs for succinct representations.

Machine learning procedures require for the most part, *feature vectors* of the same dimension, i.e., every flow has to be represented as a vector of a fixed number of carefully chosen features – i.e., information extracted from the flow.

We consider various feature-representations of *forward flows*, where a forward flow aggregates all packets, with a same *five-tuple* identifier, sent from a device being monitored to another device or server. The five-tuple identifier consists of source IP address, source port, destination IP address, destination port, and protocol. The basic representations considered are as follows.

- **STATS:** a set of statistical quantities compiled from a flow. In particular, we choose 10 of the most common such statistics in the literature (see e.g., [16]), namely, flow duration, number of packets sent per second, number of bytes per second, and the following statistics on *packet sizes* (in bytes) in a flow: mean, standard deviation, the first to third quantiles, the minimum, and maximum.
- **SIZES:** a flow is represented as a time series of packet sizes in bytes.
- **IAT:** a flow is represented as a time series of inter-arrival times between packets, i.e., elapsed time in seconds between any two packets in the flow.
- **SAMP-NUM:** a flow is partitioned into small time intervals of equal length δt , and the number of packets in each interval is recorded; thus a flow is represented as a time series of packet counts in small time intervals. Here, δt might be viewed as a choice of *sampling rate* for the time series, hence the nomenclature.
- **SAMP-SIZE:** a flow is partitioned into small time intervals of equal length δt , and the total packet size (i.e., byte count) in each interval is recorded; thus, a flow is represented as a time series of byte counts in small time intervals.

Remark that any of the above time series representations (i.e., all but STATS) might be given in time domain (which we choose by default) or in Fourier domain, in which case we append *FFT* to the representation name, i.e., IAT-FFT, SAMP-NUM-FFT, and SAMP-SIZE-FFT.

When using ML procedures for novelty detection, we have to ensure that all of the above representations result in feature-vectors of the same dimension for any given device being monitored. This is automatically the case for STATS, but not for the other representations, in light of variations in flow durations and lengths (number of packets) for a given device. To ensure that each sample has the same dimension, we select a fixed time duration for all flows corresponding to the 90th percentile of all flow lengths or durations for a device. We use this duration so as to capture the typical behavior of most device instances of a particular type. Any definition of typicality may be appropriate here, depending on the desired compactness and complexity of the corresponding representation. Using the 90th percentile of all flow durations results in a comparable number of dimensions (typically 10–30) for most of the devices that we consider in this study. Details on achieving fixed feature dimensions are given in Section 4 on experimental setup.

3 Machine Learning Models and Performance Metrics

We describe the novelty detection procedures that we evaluate in our study, as well as the performance metrics that we use to compare each of these procedures.

3.1 Novelty Detection Procedures

We consider popular novelty detection procedures from Machine Learning and Statistics, approaches based on Isolation Forests (IF), One-Class Support Vector Machines (OCSVM), Kernel Density Estimation (KDE), Gaussian Mixture Models (GMM), Principal Component Analysis (PCA), and Auto Encoders (AE). Important common aspects of all such detection procedures are as follows:

1. *Data representation as features.* Detection procedures invariably require data—here network flows—represented as a vector $X \in \mathbb{R}^d$ of d predictive features. While many procedures operate directly on that feature representation (e.g., IF, KDE, GMM), others (e.g., OCSVM, PCA, AE) remap vectors X into refined representations where certain patterns—clusters of similar network activities—might be more evident.
2. *Training and testing phase.* Detection procedures are trained in a first phase using n training datapoints $\{X_i\}_{i=1}^n$ – i.e., n copies X_i of typical values of *normal* features X (e.g., each X_i representing a normal traffic

Table 1: Data representations that are commonly used for anomaly detection.

Reference	Flow duration	IAT	SIZES	FFT of IAT and SIZES	SAMP-NUM	SAMP-SIZES
Network Intrusion Detection						
Lakshari <i>et al.</i> [10]	✓	✓	✓	✗	✗	✗
Mukar <i>et al.</i> [9]	✗	✓	✗	✗	✗	✗
Mirsky <i>et al.</i> [15]	✗	✗	✗	✗	✓	✓
IoT Anomaly Detection						
Al Jawarneh <i>et al.</i> [2]	✓	✗	✓	✗	✗	✗
Doshi <i>et al.</i> [5]	✗	✓	✓	✗	✗	✗
Meidan <i>et al.</i> [14]	✗	✓	✗	✗	✓	✓
Bhatia <i>et al.</i> [3]	✗	✗	✓	✗	✓	✗
Thamilarasu <i>et al.</i> [22]	✗	✗	✓	✗	✗	✗
DDoS Detection						
Fouladi <i>et al.</i> [6]	✗	✗	✗	✓	✗	✗
Lima <i>et al.</i> [12]	✗	✗	✓	✗	✗	✗

flow), from which they produce a *scoring function* $S(X)$; high scores $S(X)$ are expected to be typical of normal observations such as the training datapoints X_i , while low-scores would be indicative of the query X being an outlier (novelty). Subsequently, in the so-called testing phase (or deployment phase), a threshold t might be chosen so that any query X is flagged as *novelty* whenever $S(X) < t$.

Note that, in practical use cases, the right choice of threshold can be difficult since the available training data is assumed to be all *normal* making it hard to assess *false negative rates*. Instead, one might choose a threshold based on the *false positive rates* the application can tolerate, which can be estimated for each choice of t based on the *normal data* (i.e., data known to not have positive label). Related issues are discussed in Section 3.2 on performance metrics.

Normality scores in ML. In KDE or GMM, the training data is used to estimate the *density* function f of the data in \mathbb{R}^d (that is their spatial distribution), where by definition $f(x)$ is low in those regions of space that have little data. This density would then serve as a scoring function $S(X) \doteq f(X)$. IF works similarly by first partitioning the space \mathbb{R}^d into ensembles of high and low density regions, and flagging any query X as a novelty if it lies in a low density region.

On the other hand, PCA and AE work by identifying a lower-dimensional space \mathcal{X} embedded in the representation space \mathbb{R}^d on which most of the training datapoints X_i appear to lie. In PCA \mathcal{X} is a linear space, while in AE it can be highly nonlinear (using nonlinear activation functions in a neural network). The score $S(X)$ then denotes how *close* X is to \mathcal{X} with lowest scores for points farthest from \mathcal{X} .

OCSVM stands farther apart as it proceeds by first remapping all X_i 's – through a transformation $\Phi(X_i)$ into a higher dimensional feature space \mathcal{H} (possibly of infinite dimension) and then essentially identifying regions of high density in \mathcal{H} . The underlying assumption is that patterns might be more visible in \mathcal{H} , for instance, all $\Phi(X_i)$ might cluster together into a *normal* region (either a half space in \mathcal{H} or an enclosing ball; the score $S(X)$ is then lower for queries X that map as $\Phi(X)$ outside the *normal* region of \mathcal{H}).

3.2 Performance Metric

Area Under the Curve (AUC). As explained above, detection procedures flag new queries X as novel if it scores below a certain threshold t (i.e., if $S(X) < t$). Now notice a tension: the higher the threshold t , the more likely it is that all novel X are correctly detected, but unfortunately, the more likely it is also that normal datapoints are flagged as novel (a false alarm). Thus, the best performing approaches—combination of data representation and choice of detection procedure—are those that alleviate this tension, performing accurate detection while minimizing false positives.

Such tradeoffs are well captured by a Receiver Operating Characteristic (ROC) curve, which plots the detection rate against the false alarm rate as t is varied from small to large; a large area under the curve (AUC) indicates that good tradeoffs are possible under the given detection approach. We therefore adopt AUC as a sensible measure of performance.

Sensitivity to Hyperparameters. All detection procedures come with hyperparameters, i.e., configuration choices that can greatly affect performance. Important hyperparameters are e.g., bandwidth in KDE or OSCVM, number of partitions in IF, number of components in GMM, embedding dimension in PCA and AE. We therefore have to carefully pick such parameters in practice, although the right approach remains unclear, especially in *unsupervised learning* problems such as novelty detection where we typically do not have a labeled validation set to evaluate choices.

Since hyperparameter tuning in unsupervised learning remains the subject of ongoing research in Machine Learning and Statistics, *we decided to present results for the best choices of parameters*, picked a posteriori as those choices that result in the best performance on a test set, as described in Section 4.1 below.

More configuration details such as range or parameters are given in Section 4.1. Other configuration choices based on common rule-of-thumbs are covered in the appendix along with relevant results.

4 Experiment Setup

We first describe the process by which we choose hyperparameters for each of the novelty detection procedures that we evaluate in this study. We then describe the datasets we use to evaluate each novelty detection method, including how we process each of these datasets and select parameters for each corresponding feature representation.

4.1 Hyperparameter Choices for Novelty Detection Procedures

All detection procedures are implemented in the scikit-learn Python package. We now describe configuration choices, both for the best hyperparameter choice (OPT) – picked a posteriori using test data as described in Section 3.2 above – and a rule-of-thumbs choice (Default). The results in the main paper are presented for the OPT choice, while results for Default are presented in the appendix.

- OCSVM [20] (implemented by [24]). We choose a Gaussian kernel of the form $K(x, x') \propto \exp(-\|x - x'\|^2/2\sigma^2)$, and pick σ as follows. We consider the quantiles $[0.1, 0.2, \dots, 0.9] \cup \{0.95\}$ on increasing distances between pairs of points in the training sample.
OPT: The parameter σ is then picked as that quantile which yields the best AUC.
Default: σ is picked as the 0.3 quantile of inter-point distances.
- KDE [11, 21]. We use a Gaussian kernel, of the same form as OCSVM above, and pick the *bandwidth* σ exactly the same way for both **OPT** and **Default**.
- GMM [4]. We choose the number of Gaussian components k on a range $[2, 5, 8, 11, 14, 17, 20, 23, 26, 30]$.
OPT: k is chosen as the value in the range maximizing AUC.
Default: k is obtained as the number of high-density regions (or modes) in the training data, as obtained by the quickshift++ procedure of [8].
- IF [13] (implemented by [24]). We pick the number k of trees in the range 30 to 300 with increments of 10.
OPT: k is chosen as the value in the range maximizing AUC.
Default: k is 100, which is the same as the default value in pyod.
- PCA [1] For $X \in \mathbb{R}^d$, i.e., having d features, we pick the projection dimension dim in a range. We pick dim in a range $\{\lceil 1 + i \cdot (d - 2)/9 \rceil\}_{i=0}^9$ of (up to 10) values (approximately evenly spaced) between 1 and $d - 1$.
OPT: dim is chosen as the value in the range maximizing AUC.
Default: dim is estimated by maximum likelihood (MLE) in scikit-learn.
- AE [25] (from PyTorch [18] using LeakyRelu for activation functions). For $X \in \mathbb{R}^d$, we use the following architecture with 5 layers, determined by a tuning parameter dim : one input layer of size d (number of *neurons*), followed by a hidden layer of size $\text{h-dim} \doteq \min\{(d - 1), \lceil 2 \cdot \text{dim} \rceil\}$, a latent layer of size dim , a subsequent hidden layer of size h-dim , and finally an output layer of size d . We pick dim in a range $\{\lceil 1 + i \cdot (d - 2)/9 \rceil\}_{i=0}^9$ of (up to 10) values (approximately evenly spaced) between 1 and $d - 1$.
OPT: dim is chosen as the value in the range maximizing AUC.
Default: dim is $\lceil d/2 \rceil$.

Table 2: Datasets.

Reference	Description	Devices	Type of Novelty
UNB IDS [17]	Normal and DDoS attack traces from personal computers (PC), which are chosen from Monday trace and Friday trace.	Five PCs (noted as PC1, PC2, PC3, PC4, and PC5, respectively)	DDoS attack
CTU IoT [23]	Bitcoin-Mining and Botnet traffic traces generated by two Raspberries; we aim to distinguish the two devices by their attack traces (i.e., Mirai and CoinMiner); hence we use one generated Mirai as <i>normal</i> , the other generated CoinMiner as <i>novel</i> .	Two Raspberries	Novel (infected) device
MAWI [7]	Normal traffic generated by two PCs, which are collected on Dec. 07, 2019; we use one PC (whose IP address is 202.171.168.50) as <i>normal</i> , the other (whose IP address is 202.4.27.109) as <i>novel</i> .	Two PCs	Novel (normal) device
Lab IoT	Data traces are generated by IoT devices (e.g., fridge) in a private lab environment. We choose two kinds of normal traffic generated by a smart TV and a PC.	A smart TV and a PC (noted as TV&PC)	Novel device
	Four smart-home devices, each with two types of traffic traces labeled as <i>normal</i> when there is no human interaction, and <i>novel</i> when being operated by a human.	Google home (GHom), Samsung camera (SCam), Samsung fridge (SFrig), and Bose soundtouch (BSTch)	Novel activity

4.2 Data

We consider a combination of publicly available traffic traces and traces collected on private consumer IoT devices. We aim to evaluate representative set of devices, from multi-purpose devices such as laptop PCs, and Google Home, to less complex electronics and appliances such as smart cameras and TVs. Furthermore we aim at a representative set of novelty, from benign novelties (new activity, or a new device type), to novelties due to malicious activities (DDoS attack). Table 2 describes these datasets, and types of novelty being detected.

Obtaining flows. We parse upstream flows from datasets in Table 2 using Scapy [19]. Given that certain devices can have arbitrarily long flows, we truncate each flow from a given dataset to have duration at most that of the 90th upper-percentile of flow durations in the dataset. Henceforth, a *flow* refers to these choices of flows involving truncation.

Selecting feature representation dimension. Each flow is then represented using any of the feature-representation choices described in Section 2. Here, we have to ensure that, given a representation choice, e.g., IAT, all flows result in vectors of the same dimension d for each dataset. We apply a similar approach to enforce such fixed dimension d , as outlined below. For a fixed dataset, let d_0 denote the 90th upper-percentile of number of packets per flow.

- **STATS:** automatically results in vectors of the same dimension d , equal to the number of statistics (on packet size) computed on a flow.
- **IAT, or SIZE:** dimension is fixed to $d = d_0 - 1$ for IAT, and $d = d_0$ for size; namely, for long flows, we truncate the number of packets in a flow to the first d_0 ; for short flows where the number of packets is less than d_0 , we append 0's to the IAT representation to arrive at d features.
- **IAT + SIZE:** just concatenates IAT and SIZE representations to dimension $d = 2d_0 - 1$.
- **SAMP-NUM or SAMP-SIZE:** dimension is fixed to $d = d_0 - 1$ as in the case of IAT. Now we pick a fixed window size δt , and each flow is divided into up to d windows of length δt ; for flows of short duration, where δt is large w.r.t. duration, we simply append 0's.

Choice of δt : we start with candidate choices $\Delta \doteq \{t_f/d\}$, over durations t_f of flows f in a given dataset. We then consider 10 choices of δt in Δ , each choice an i -th quantile of values in Δ , for each $i \in \{10, 20, 30, 40, 50, 60, 70, 80, 90, 95\}$. Thus, each such choice of δt yields one (SAMP-NUM or SAMP-SIZE) representation for all flows; since we do not know which such representation (i.e. choice of δt) is best a priori² we report the best AUC resulting out of all 10 choices of δt .

Each of the above representations, besides STATS, can then be viewed as fixed length time series, and therefore admit a Fourier domain representation; the corresponding Fourier representation is then set to the same dimension d , i.e., we retain as many Fourier components as the original time series.

The resulting representation dimensions for each dataset are reported in Table 4 in the appendix.

5 Results

In this section, we explore how data representation affects the performance of different novelty detection algorithms. We are interested in the difference in AUC due to the presence or absence of particular feature types with respect to a set of basic feature representations, namely STATS, SIZE, IAT, SUMP-NUM, and SAMP-SIZE (Table 3 also includes IAT+SIZE as a baseline for future comparisons). We will see that across ML procedures, (1) Fourier domain representations have little advantage over raw time series (despite being generally thought of as a better way to capture important trends in timeseries), while the effect of (2) packet size information, and (3) packet header information tend to be significant overall. We focus on some of the most popular ML approaches (OCSVM, IF, AE, KDE) in the main text, under **OPT** tuning, while results for omitted ML approaches, for **Default** tuning, and omitted datasets are given in the appendix. We substantiate messages (1), (2), and (3) in subsections 5.1, 5.2, and 5.3. Table 3 gives baselines for comparisons.

Statistical significance. Throughout this section, we often display error bars of length $1/\sqrt{n}$ (n denoting test sample sizes as given in Table 5), which is a ballpark for standard deviation in AUC computed on a test sample of size n .

We first explore the effect of Fourier domain representations; then we explore how including packet sizes and fields from the packet header ultimately affect the performance of different novelty detection approaches.

5.1 Effect of Fourier Domain Representation

We compare Fourier domain representations—obtained by *Fast Fourier Transforms* (FFT), where we retain as many FFT components as the number of time points—to raw time-domain representations of each flow IAT, SAMP-NUM, SAMP-SIZE. Figure 1 presents the difference in AUC, i.e., the AUC obtained under FFT minus that obtained under the corresponding raw time series representation.

The same trend is observed across ML procedures: apart for a few device datasets (e.g., positive effect in SFrig and negative effect in BSTch w.r.t. IAT), FFT makes no significant difference in the achieved AUC over raw time series. In other words, the various ML procedures seem able to extract much of the same information already from the raw time series, i.e., their *internal representations* of the data already account for major trends in the times series and thus do away with the need to preprocess through FFT.

Henceforth, we focus attention on raw representations for time series in subsequent discussions.

5.2 Effect of Packet Size Information

Referring back to Table 3, packet size information immediately appears to be important based on the generally higher AUCs achieved under STATS (which primarily compiles statistics on packet sizes in a flow) to those achieved under basic representations such as IAT and SAMP-NUM (devoid of packet size information). Interestingly, SIZE, a time series of packet sizes in a flow, does not perform as well as STATS does over IAT, and SAMP-NUM.

As it turns out, adding packet size information to IAT or SAMP-NUM representations improves on such representations alone. Namely, in the case of IAT, size information is added in by concatenating IAT and SIZE vectors, which we denote IAT+SIZE. For SAMP-NUM, a time-series of *number of packets* in small fixed time intervals δt , size information is accounted for by instead compiling *total packet size* in fixed time intervals δt .

²In fact we do not know how such choice might be automated in practice, as automating *sampling rates* remains an largely open research problem.

Table 3: AUCs for 4 ML approaches on basic feature representations.

Detector	Dataset	STATS	SIZE	IAT	IAT+ SIZE	SAMP- NUM	SAMP- SIZE
OCSVM	UNB(PC1)	0.56	0.70	0.78	0.92	0.74	0.76
	UNB(PC4)	0.48	0.66	0.82	0.80	0.81	0.79
	CTU	0.98	0.97	0.95	0.96	0.88	0.88
	MAWI	0.88	0.71	0.58	0.43	0.60	0.61
	TV&PC	1.00	1.00	0.96	0.99	0.95	0.93
	SFrig	0.98	0.93	0.81	0.85	0.96	0.95
	BSTch	0.97	0.99	0.97	0.99	0.96	0.95
IF	UNB(PC1)	0.49	0.49	0.51	0.74	0.66	0.70
	UNB(PC4)	0.49	0.51	0.62	0.65	0.81	0.79
	CTU	0.94	0.93	0.81	0.88	0.83	0.85
	MAWI	0.86	0.70	0.54	0.67	0.56	0.55
	TV&PC	0.95	0.98	0.90	0.99	0.74	0.79
	SFrig	0.96	0.96	0.56	0.94	0.93	0.93
	BSTch	0.97	0.98	0.94	0.98	0.98	0.96
AE	UNB(PC1)	0.72	0.40	0.50	0.93	0.81	0.77
	UNB(PC4)	0.70	0.52	0.64	0.84	0.83	0.86
	CTU	0.91	0.96	0.85	0.96	0.83	0.87
	MAWI	0.56	0.58	0.50	0.70	0.58	0.55
	TV&PC	1.00	1.00	0.97	0.99	0.85	0.95
	SFrig	0.95	0.85	0.72	0.92	0.96	0.96
	BSTch	0.97	0.93	0.98	0.99	0.96	0.96
KDE	UNB(PC1)	0.34	0.58	0.68	0.92	0.74	0.76
	UNB(PC4)	0.47	0.63	0.76	0.80	0.81	0.85
	CTU	0.96	0.93	0.94	0.97	0.82	0.84
	MAWI	0.88	0.48	0.57	0.43	0.60	0.57
	TV&PC	1.00	1.00	0.96	0.99	0.88	0.93
	SFrig	0.97	0.91	0.79	0.78	0.95	0.95
	BSTch	0.97	0.98	0.95	0.98	0.95	0.95

Figure 2 presents the differences in AUC obtained using packet size information, minus those obtained on corresponding representations without size information. We observe significant positive differences for most ML procedures on most datasets—which correspond to a range of novelty detection problems, whether malicious attacks, or novel devices or activity. Even in those cases when size information does not help, it nonetheless does not hurt, except in rare cases such as MAWI under IAT when employing OCSVM and KDE. However, even in this case, we observe (see Table 3) that the concatenation of IAT+SIZE yields *worse* AUC than IAT or SIZE alone. The exact reason is unclear and could be due to *overfitting*, as the concatenation increases feature dimension in ways that might affect *nonparametric* models such as OCSVM and KDE given the relatively modest training size of MAWI (800+ datapoints).

The most significant positive differences are observed for IF, AE, and PCA in the case of IAT, while no significant differences are observed for sampling-based representations, such as SAMP-SIZE vs. SAMP-NUM. Interestingly, for fixed datasets, trends are generally consistent across ML methods, suggesting that whether size information helps depends most on devices’ characteristics, rather than the ML method employed or the type of detection problem.

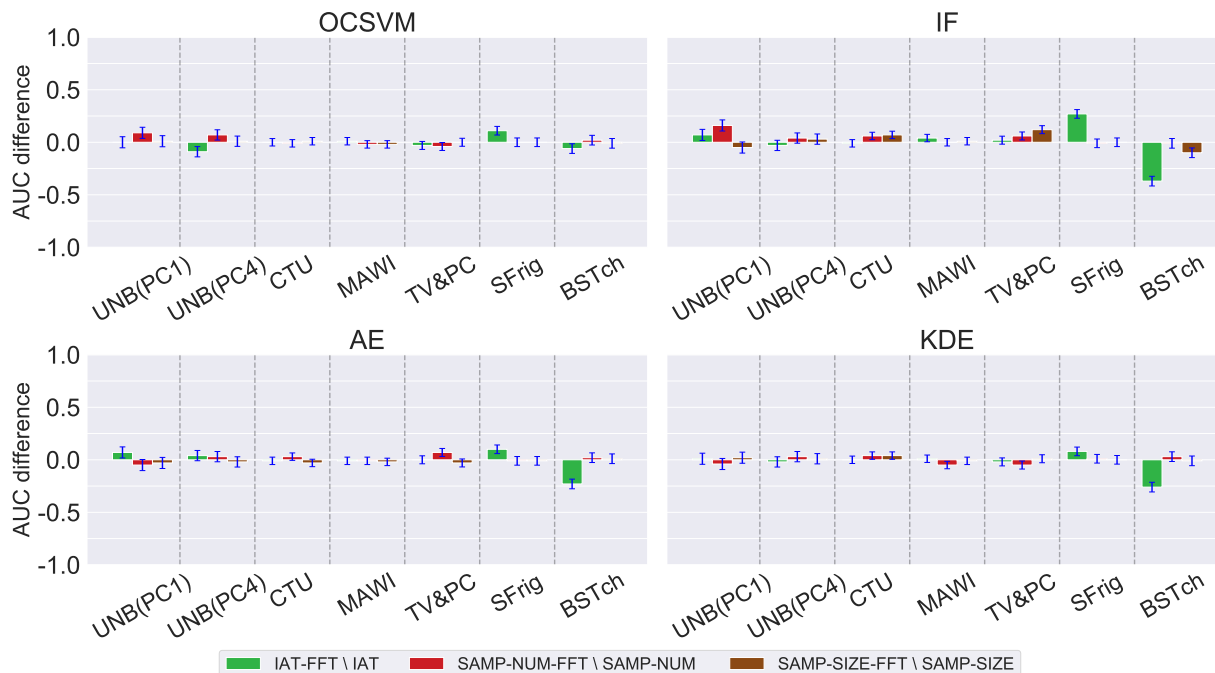


Figure 1: Difference in AUC for FFT vs. raw time series representations.

In general, the inclusion of packet sizes for novelty detection makes sense, as the packet size can provide some indication about the nature of the underlying activity. For example, for the case of the UNB dataset, attack traffic may be unique in size relative to other types of activities. In the case of the private IoT datasets, novel activities may be less likely to produce individual packets of differing sizes unless the activities themselves are new.

5.3 Effect of Packet Header

We now consider the effects of information in packet headers on novelty detection, focusing on the information available in various TCP flags. We focus on the following eight flags in each packet: FIN, SYN, RST, PSH, ACK, URG, ECE, and CWR, and TTL. We do not include IP address or port information in this part of our analysis. Given the already established benefits (or at least invariance in AUC) of including packet size information, we now take representations such as STATS, IAT+SIZE and SAMP-SIZE as baselines to which we concatenate packet header information (for each packet in a flow) and record differences in performance.

In general, we observe no significant degradation in performance in adding header information, and in fact, observe improvements for some datasets such as SFrig under OCSVM and KDE (novel activity detection) where we might not necessarily expect such header information to help. The simple explanation is that in fact, even for problems such as activity detection, a device might switch destination IP or ports depending on the type of activity being performed.

Figure 3 presents the differences in AUC obtained with packet header information minus that obtained without header information. The same trends are observed across ML approaches. As might be expected, we observe the most significant improvements on those datasets corresponding to (1) detecting malicious activity (UNB)—where infected traffic might be rerouted to new destinations, thereby resulting in traffic with different distributions of packet TTL values corresponding to the different, new destinations—or (2) detecting novel devices (CTU, MAWI)—where header information such as certain TCP options can a device or operating system pertinent to a device.

Although TV & PC seem to be an exception to (2), the general lack of improvement is simply due to the fact that AUC’s for the baseline representations were already near perfect (close to 1) across ML approaches (see Table 3). This happens to also be the case (i.e., near perfect AUC’s) for those baseline representations where we observe little difference in AUC for the two detection problems (1) and (2). The most improvement across ML methods is observed for MAWI where the baseline representations yielded poor AUC’s to start with (Table 3).

Figure 4 shows that certain packet header fields can be particularly useful for novelty detection, depending on the anomaly; these results are evident in the results. One of the more important findings from taking a closer look at the

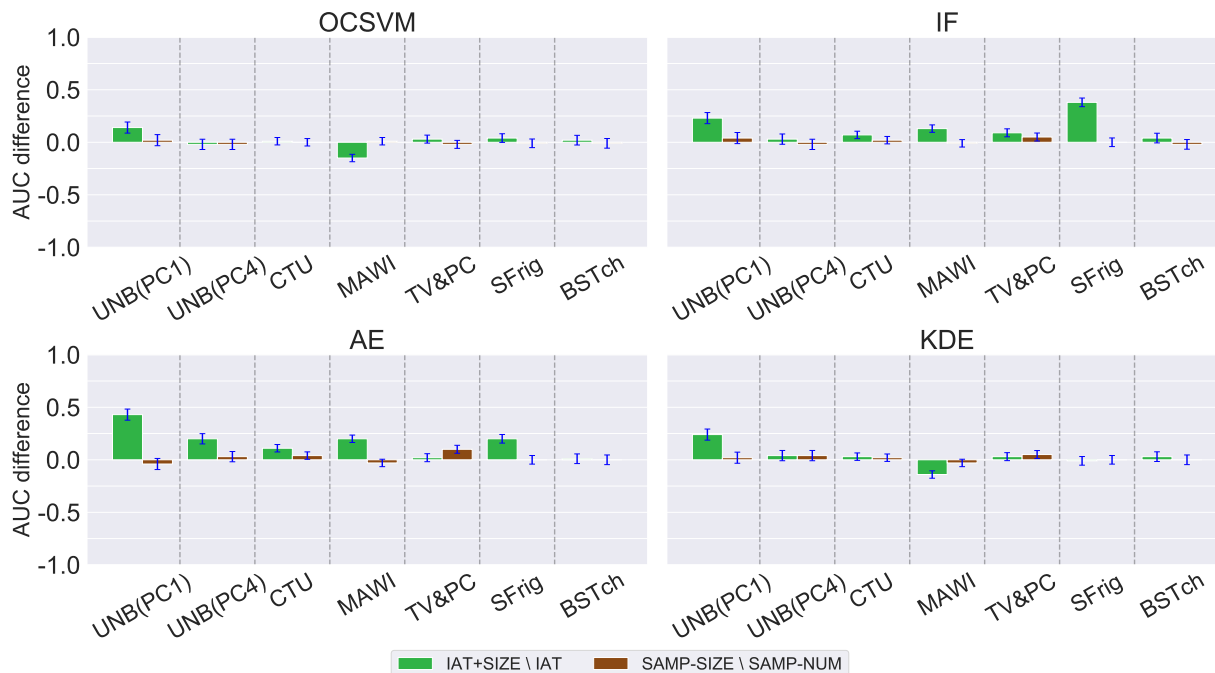


Figure 2: Differences in AUC due to including vs. excluding packet size information.

correlations between features and ground truth is that the most important packet header values will *depend on the novelty detection problem*. We explore this in more detail below.

Attack detection. In the case of the UNB dataset, we see that the SYN flag can be very useful in identifying novelty events related to security, as the SYN flag correspond to a TCP handshake that occurs at the beginning of the connection and is commonly related to certain types of denial of service attacks, such as a SYN flood. Other packet header information that exhibits correlation include other flags that are commonly associated with denial of service attacks, including the RST and FIN flags, which victim hosts may send in response to a SYN. In all of these cases, an increase in packets that include these flags could likely correspond with a volumetric denial of service attack, such as a SYN flood.

Novel device detection. The MAWI dataset, where the novelty detection problem involves detecting a novel device, finds the TTL field in a packet header to be significant. This also follows intuition, as the TTL value is a coarse indicator of network topology (i.e., how many network-level “hops” a device is from a particular destination endpoint) and naturally two different devices on the network may be located at different network attachment points and thus be different distances away from common network locations. Such topological differences would be apparent in the TTL field, and a new device attaching at a different location on the network could appear as a sudden influx of network traffic that bears a different distribution in TTL values. In particular, sudden deviations in distributions of TTL values in the dataset may thus reflect the injection of traffic from new devices, or possibly attackers. On the other hand, we see in this dataset that the SYN and TTL fields are less useful for novelty detection concerning activities (e.g., the SFrig dataset, which involves detection of activities in the dataset).

Novel activity detection. If someone begins to interact with a connected IoT device in new ways—triggering new types of activities—the traffic itself may bear differences from previously seen traffic. Differences in the traffic itself may arise because activities themselves may bear unique signatures in the underlying network traffic. For example, the amount and nature of traffic generated by opening and closing a refrigerator door in SFrig will generate different types of traffic than the kind of traffic that is generated by activities that do not involve human interaction (e.g., a software update). These fundamental differences may appear in different ways, such as differences in traffic volume or timing, and in some cases they may appear in the TCP header flags themselves. In the case of SFrig, we see that the ACK flag has a high correlation with ground truth, indicating that changes in the prevalence of ACKs (i.e., packet acknowledgments) may represent changes in underlying activities. This characteristic likely results from the underlying behavior of TCP, the Internet’s transport protocol, and how it handles packet acknowledgments for flows of different sizes and timings. For example, for large traffic flows, TCP will sometimes optimize its acknowledgment behavior,

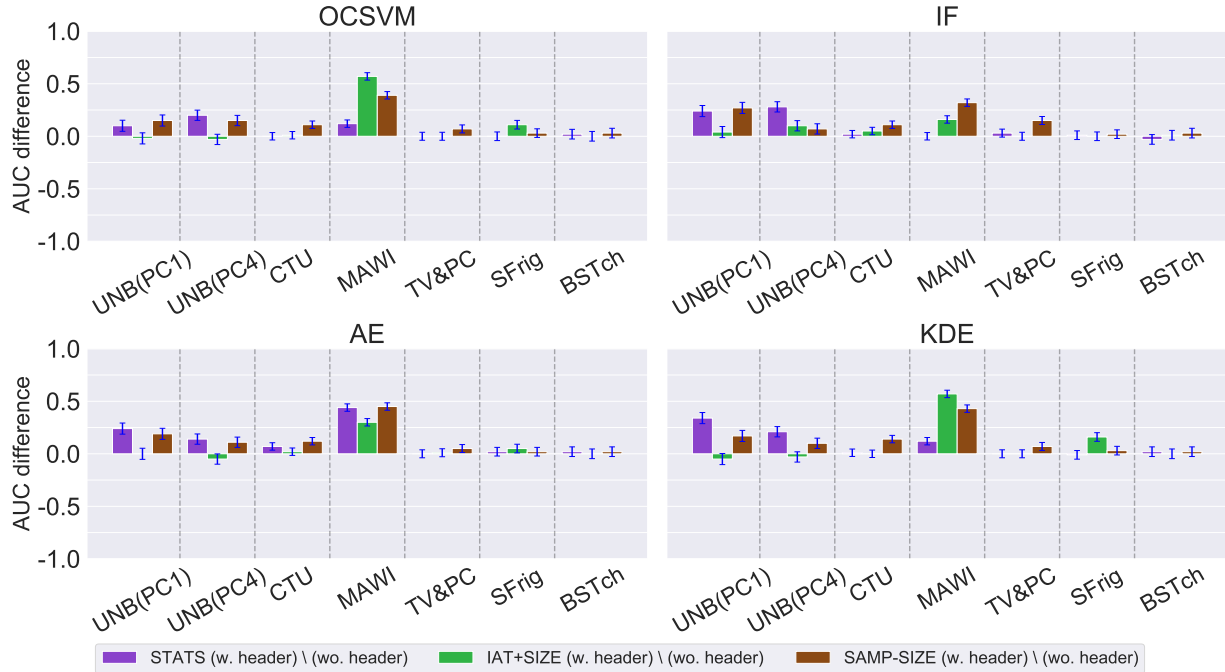


Figure 3: Differences in AUC due to including vs. excluding packet header information.

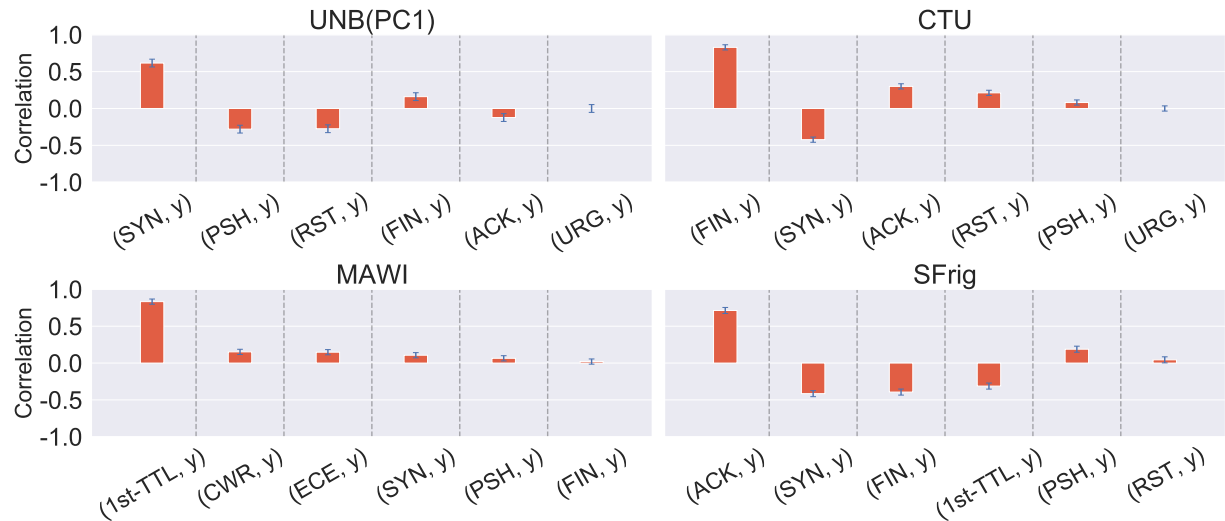


Figure 4: Top 6 correlation between each value in packet headers and ground truth (y).

using techniques such as *delayed ACK* to improve network performance. Highly interactive behavior and the traffic it generates may exhibit very different qualities than automated traffic (e.g., a software update involving the transfer of a large amount of data) and thus different behavior in ACK traffic. The distribution of ACK fields in the traffic may reflect higher traffic volumes during periods of novel activity.

6 Conclusion

Novelty detection problems in computer networking require making important decisions about how to represent traffic data. Traffic data are captured as “raw” packet captures, where each packet has an individual timestamp, thus taking the format of an irregularly sampled timeseries. The data itself must be subsequently transformed into a representation for

model input; often, the representation of the input data can be as important for model accuracy as the choice of the model or model parameters.

This paper takes a first step towards exploring the effects of network traffic representation for novelty detection, focusing on a range of novel behaviors in the Internet of Things (IoT)—security events, novel devices, and novel human behaviors and interactions. We use a collection of datasets to evaluate different traffic representations across a range of models. Our work reveals several important findings: (1) popular Fourier domain representations do not significantly improve accuracy over simple time-domain representations; (2) representations that include traffic sizes and packet header fields (e.g., IP TTL, TCP flags) can significantly improve model accuracy as measured by area under the curve (AUC).

This study has important implications for the design of future measurement and analysis systems that use network traffic data for novelty detection, in the IoT and more generally for deployed network systems. From a systems perspective, capturing full packet traces can introduce significant costs, yet aggressive aggregation can preclude certain data representations that are important for model accuracy. In particular, we find that raw packet traces can be summarized in terms of flow-level statistics in short time windows or inter-arrival times, and augmented with sequences of packet sizes and flags; augmentation of simple timeseries representations with this metadata significantly improves accuracy.

Acknowledgements

This work was supported by NSF Award CPS-1953740 and a Siebel Energy Institute grant.

References

- [1] C. C. Aggarwal. Outlier analysis. In *Data mining*, pages 237–263. Springer, 2015.
- [2] S. A. Aljawarneh and R. Vangipuram. Garuda: Gaussian dissimilarity measure for feature representation and anomaly detection in internet of things. *The Journal of Supercomputing*, pages 1–38, 2018.
- [3] R. Bhatia, S. Benno, J. Esteban, T. Lakshman, and J. Grogan. Unsupervised machine learning for network-centric anomaly detection in iot. In *Proceedings of the 3rd ACM CoNEXT Workshop on Big Data, Machine Learning and Artificial Intelligence for Data Communication Networks*, pages 42–48, 2019.
- [4] C. M. Bishop. *Pattern recognition and machine learning*. springer, 2006.
- [5] R. Doshi, N. Apthorpe, and N. Feamster. Machine learning ddos detection for consumer internet of things devices. In *2018 IEEE Security and Privacy Workshops (SPW)*, pages 29–35. IEEE, 2018.
- [6] R. F. Fouladi, C. E. Kayatas, and E. Anarim. Frequency based ddos attack detection approach using naive bayes classification. In *2016 39th International Conference on Telecommunications and Signal Processing (TSP)*, pages 104–107. IEEE, 2016.
- [7] T. M. W. Group. "mawi wide dataset". <https://mawi.wide.ad.jp/mawi/>. Accessed: 2019-12-13.
- [8] H. Jiang, J. Jang, and S. Kpotufe. Quickshift++: Provably good initializations for sample-based mean shift. *arXiv preprint arXiv:1805.07909*, 2018.
- [9] A. Kumar, A. Abdelhadi, and C. Clancy. Novel anomaly detection and classification schemes for machine-to-machine uplink. In *2018 IEEE International Conference on Big Data (Big Data)*, pages 1284–1289. IEEE, 2018.
- [10] A. H. Lashkari, A. F. A. Kadir, L. Taheri, and A. A. Ghorbani. Toward developing a systematic approach to generate benchmark android malware datasets and classification. In *2018 International Carnahan Conference on Security Technology (ICCST)*, pages 1–7. IEEE, 2018.
- [11] L. J. Latecki, A. Lazarevic, and D. Pokrajac. Outlier detection with kernel density functions. In *International Workshop on Machine Learning and Data Mining in Pattern Recognition*, pages 61–75. Springer, 2007.
- [12] F. S. d. Lima Filho, F. A. Silveira, A. de Medeiros Brito Junior, G. Vargas-Solar, and L. F. Silveira. Smart detection: An online approach for dos/ddos attack detection using machine learning. *Security and Communication Networks*, 2019, 2019.
- [13] F. T. Liu, K. M. Ting, and Z.-H. Zhou. Isolation-based anomaly detection. *ACM Transactions on Knowledge Discovery from Data (TKDD)*, 6(1):3, 2012.
- [14] Y. Meidan, M. Bohadana, Y. Mathov, Y. Mirsky, A. Shabtai, D. Breitenbacher, and Y. Elovici. N-baiot—network-based detection of iot botnet attacks using deep autoencoders. *IEEE Pervasive Computing*, 17(3):12–22, 2018.
- [15] Y. Mirsky, T. Doitshman, Y. Elovici, and A. Shabtai. Kitsune: an ensemble of autoencoders for online network intrusion detection. *arXiv preprint arXiv:1802.09089*, 2018.
- [16] A. Moore, D. Zuev, and M. Crogan. Discriminators for use in flow-based classification. *Queen Mary and Westfield College, Department of Computer Science*, (August), 2005.
- [17] T. U. of New Brunswick. The CICIDS2017 Dataset. <https://www.unb.ca/cic/datasets/ids-2017.html>, 2017. Accessed: 2019-12-13.
- [18] A. Paszke, S. Gross, F. Massa, A. Lerer, J. Bradbury, G. Chanan, T. Killeen, Z. Lin, N. Gimelshein, L. Antiga, A. Desmaison, A. Kopf, E. Yang, Z. DeVito, M. Raison, A. Tejani, S. Chilamkurthy, B. Steiner, L. Fang, J. Bai, and S. Chintala. Pytorch: An imperative style, high-performance deep learning library. In H. Wallach, H. Larochelle, A. Beygelzimer, F. d'Alché-Buc, E. Fox, and R. Garnett, editors, *Advances in Neural Information Processing Systems 32*, pages 8024–8035. Curran Associates, Inc., 2019.
- [19] Scapy. "scapy". <https://scapy.net/index>. Accessed: 2019-12-13.
- [20] B. Schölkopf, R. C. Williamson, A. J. Smola, J. Shawe-Taylor, and J. C. Platt. Support vector method for novelty detection. In *Advances in neural information processing systems*, pages 582–588, 2000.
- [21] D. W. Scott and S. R. Sain. Multidimensional density estimation. *Handbook of statistics*, 24:229–261, 2005.
- [22] G. Thamarasu and S. Chawla. Towards deep-learning-driven intrusion detection for the internet of things. *Sensors*, 19(9):1977, 2019.
- [23] C. T. University. "malware on iot dataset". <https://www.stratosphereips.org/datasets-iot>. Accessed: 2019-12-13.

- [24] Y. Zhao, Z. Nasrullah, and Z. Li. Pyod: A python toolbox for scalable outlier detection. *Journal of Machine Learning Research*, 20(96):1–7, 2019.
- [25] C. Zhou and R. C. Paffenroth. Anomaly detection with robust deep autoencoders. In *Proceedings of the 23rd ACM SIGKDD International Conference on Knowledge Discovery and Data Mining*, pages 665–674. ACM, 2017.

A Information on Datasets

Table 4: Data representation dimensions for each dataset.

Device	IAT, IAT-FFT	SIZE, SIZE-FFT	STATS	SAMP-NUM, SAMP-NUM-FFT, SAMP-SIZE
PC1	14	15	10	14
PC2	16	17	10	16
PC3	15	16	10	15
PC4	17	18	10	17
PC5	17	18	10	17
2Rsps	8	9	10	8
2PCs	25	26	10	25
TV&PC	12	13	10	12
GHom	19	20	10	19
SCam	6	7	10	6
SFrig	30	31	10	30
BSTch	148	149	10	148

Table 5: Train and Test sample set sizes.

Reference	Devices	Train set size	Test set sizes
UNB IDS	PC1	Normal: 10000	Normal: 179, Attack: 179
	PC2	Normal: 10000	Normal: 257, Attack: 257
	PC3	Normal: 10000	Normal: 221, Attack: 221
	PC4	Normal: 10000	Normal: 209, Attack: 209
	PC5	Normal: 10000	Normal: 360, Attack: 360
CTU IoT	2Rsps	Normal: 3991	Normal: 400, Novel device: 400
MAWI	2PCs	Normal: 824	Normal: 400, Novel device: 400
Private IoT	TV&PC	Normal: 4636	Normal: 346, Novel device: 346
	GHom	Normal: 7376	Normal: 513, Novel activity: 513
	SCam	Normal: 10000	Normal: 197, Novel activity: 197
	SFrig	Normal: 2952	Normal: 296, Novel activity: 296
	BSTch	Normal: 997	Normal: 236, Novel activity: 236

B Evaluation with Best Parameters

Table 6: AUCs for 4 ML approaches on basic feature representations with best parameters.

Detector	Dataset	STATS	SIZE	IAT	IAT+ SIZE	SAMP- NUM	SAMP- SIZE
OCSVM	UNB(PC2)	0.64	0.75	0.82	0.81	0.82	0.85
	UNB(PC3)	0.59	0.85	0.87	0.88	0.83	0.85
	UNB(PC5)	0.47	0.73	0.84	0.86	0.76	0.81
	GHom	0.76	0.97	0.70	0.70	0.95	0.96
	SCam	0.58	0.61	0.56	0.62	0.56	0.61
IF	UNB(PC2)	0.68	0.61	0.68	0.75	0.81	0.80
	UNB(PC3)	0.62	0.63	0.70	0.79	0.81	0.80
	UNB(PC5)	0.55	0.61	0.69	0.74	0.79	0.74
	GHom	0.88	0.77	0.44	0.54	0.96	0.96
	SCam	0.52	0.51	0.53	0.54	0.60	0.56
AE	UNB(PC2)	0.78	0.66	0.71	0.83	0.83	0.77
	UNB(PC3)	0.76	0.58	0.71	0.90	0.85	0.80
	UNB(PC5)	0.82	0.66	0.73	0.87	0.88	0.87
	GHom	0.84	0.69	0.35	0.86	0.97	0.96
	SCam	0.63	0.61	0.57	0.65	0.61	0.60
KDE	UNB(PC2)	0.61	0.73	0.82	0.80	0.81	0.80
	UNB(PC3)	0.53	0.84	0.84	0.87	0.82	0.85
	UNB(PC5)	0.53	0.69	0.84	0.86	0.75	0.82
	GHom	0.60	0.97	0.71	0.72	0.96	0.96
	SCam	0.52	0.50	0.56	0.63	0.54	0.60

Table 7: AUCs for GMM and PCA on basic feature representations with best parameters.

Detector	Dataset	STATS	SIZE	IAT	IAT+ SIZE	SAMP- NUM	SAMP- SIZE
GMM	UNB(PC1)	0.55	0.59	0.62	0.75	0.84	0.74
	UNB(PC2)	0.84	0.72	0.71	0.74	0.83	0.84
	UNB(PC3)	0.87	0.78	0.75	0.91	0.83	0.81
	UNB(PC4)	0.68	0.59	0.61	0.65	0.89	0.86
	UNB(PC5)	0.60	0.64	0.72	0.79	0.85	0.76
	CTU	0.98	0.96	0.90	0.93	0.91	0.88
	MAWI	0.80	0.63	0.53	0.59	0.62	0.69
	TV&PC	1.00	1.00	0.97	0.99	0.99	0.99
	GHom	0.96	0.93	0.90	0.93	0.97	0.96
	SCam	0.62	0.61	0.59	0.63	0.63	0.65
	SFrig	0.97	0.97	0.95	0.97	0.96	0.95
	BSTch	0.99	0.99	0.98	0.99	0.98	0.97
	PCA	UNB(PC1)	0.74	0.41	0.35	0.93	0.86
UNB(PC2)		0.86	0.67	0.71	0.82	0.85	0.81
UNB(PC3)		0.75	0.56	0.70	0.88	0.83	0.82
UNB(PC4)		0.72	0.52	0.65	0.82	0.89	0.88
UNB(PC5)		0.79	0.64	0.73	0.87	0.91	0.89
CTU		0.95	0.95	0.84	0.97	0.84	0.87
MAWI		0.66	0.71	0.49	0.74	0.59	0.54
TV&PC		1.00	1.00	0.96	1.00	0.94	0.94
GHom		0.85	0.71	0.34	0.97	0.97	0.96
SCam		0.63	0.61	0.57	0.65	0.62	0.59
SFrig		0.97	0.95	0.79	0.97	0.96	0.96
BSTch		0.96	0.98	0.99	0.99	0.97	0.97

B.1 Effect of Fourier Domain Representation

The figures below show the difference in AUC for the FFT vs. raw timeseries representations with the best model parameters for each model. FFT transformations have little effect on model accuracy.

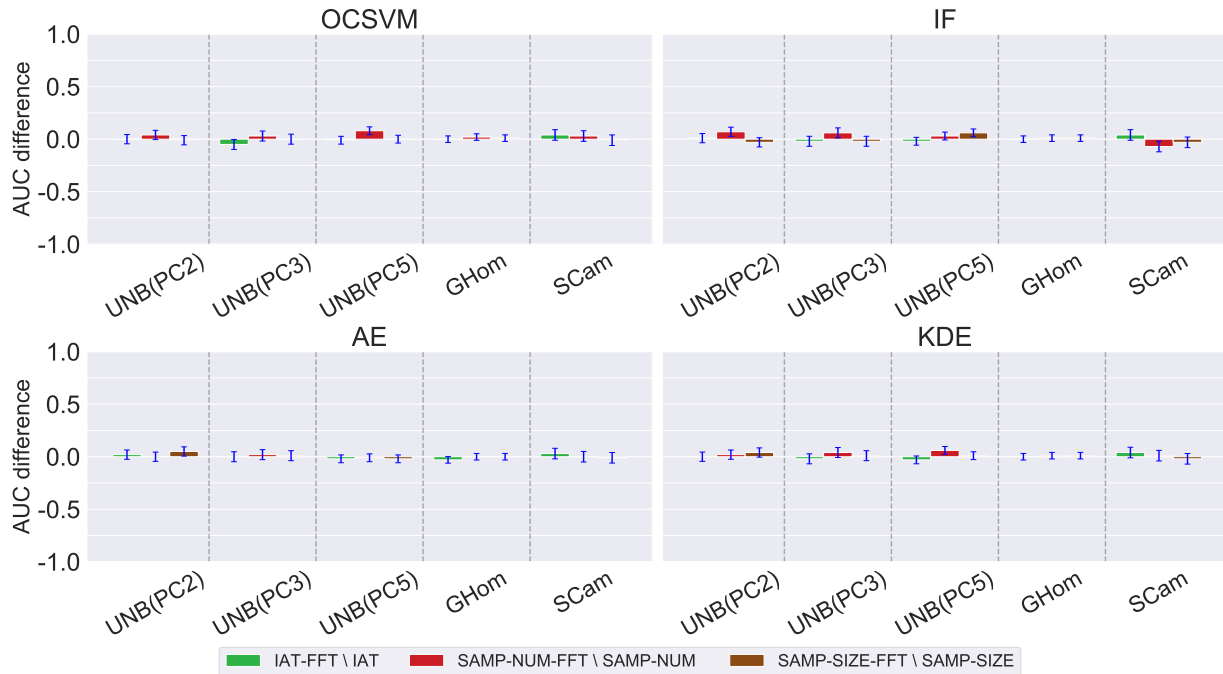


Figure 5: Difference in AUC for FFT vs. raw time series representations with best parameters.

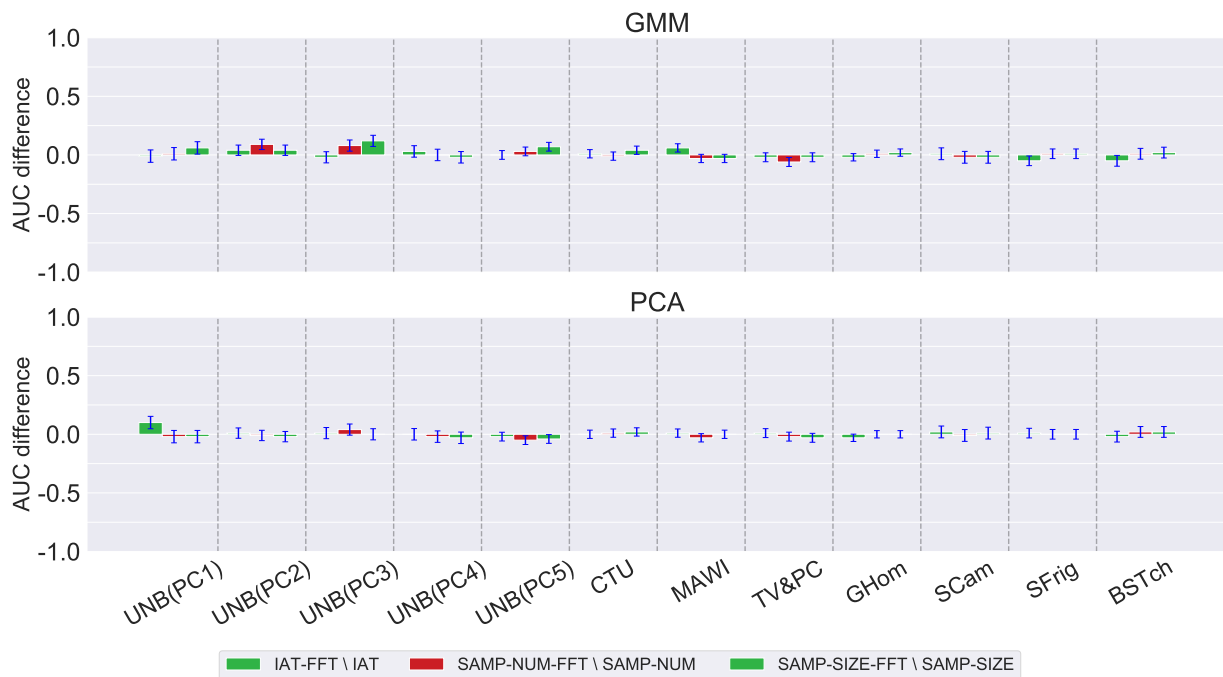


Figure 6: Difference in AUC for FFT vs. raw time series representations generated by GMM and PCA with best parameters.

B.2 Effect of Packet Size Information

The figures below show the difference in AUC for including vs. excluding packet size information for different models: IAT and SAMP. Including packet size can significantly improve model accuracy in certain cases.

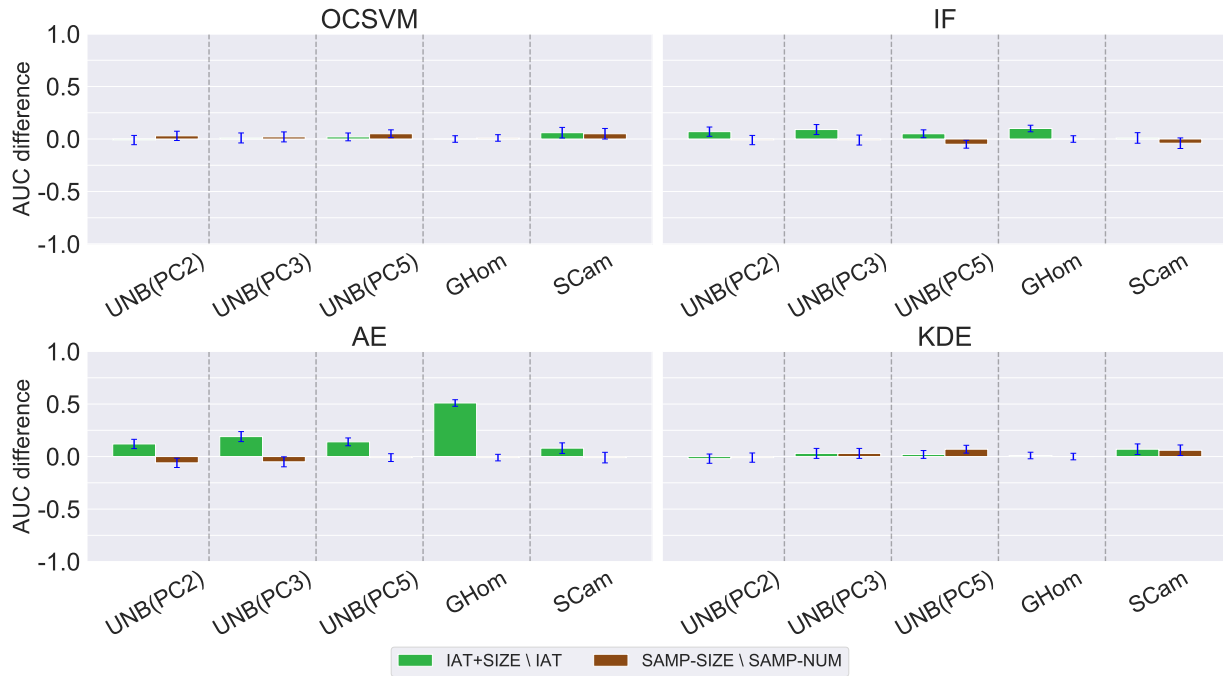


Figure 7: Differences in AUC due to including vs. excluding packet size information with best parameters.

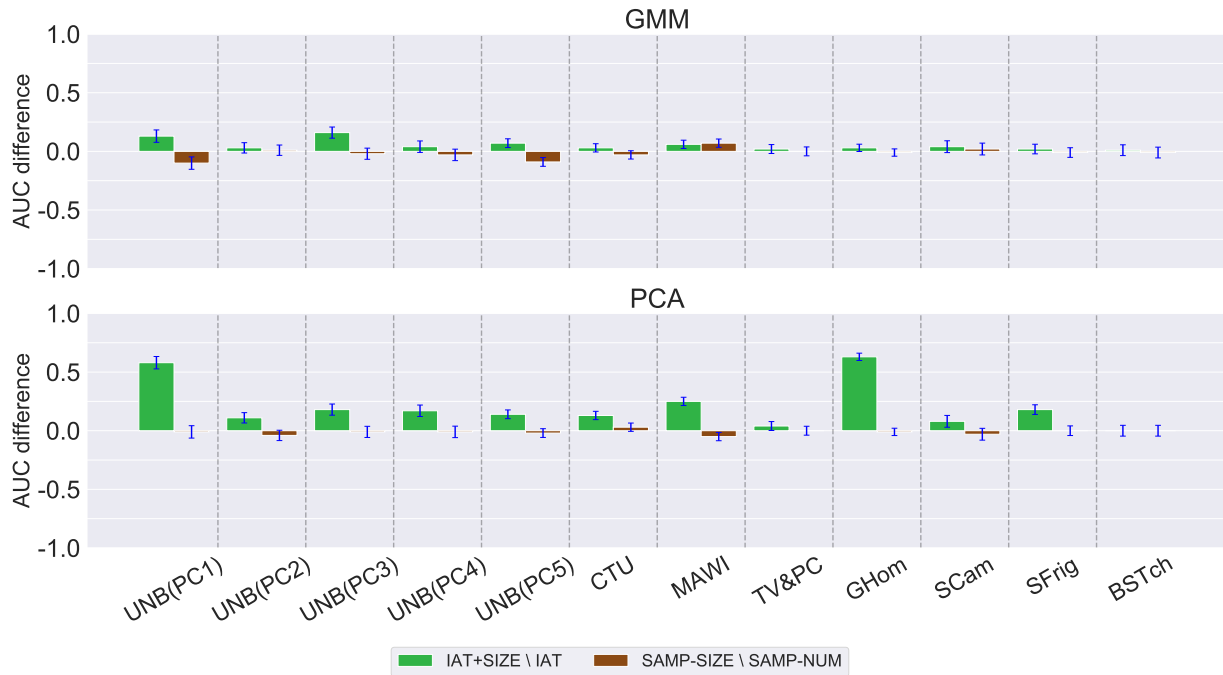


Figure 8: Differences in AUC due to including vs. excluding packet size information generated by GMM and PCA with best parameters.

B.3 Effect of Packet Header

The figures below show the difference in AUC for including vs. excluding packet header information (i.e., IP TTL, TCP flags) for different models: STATS, IAT, and SAMP. Including packet header information almost always improves model accuracy for these models.

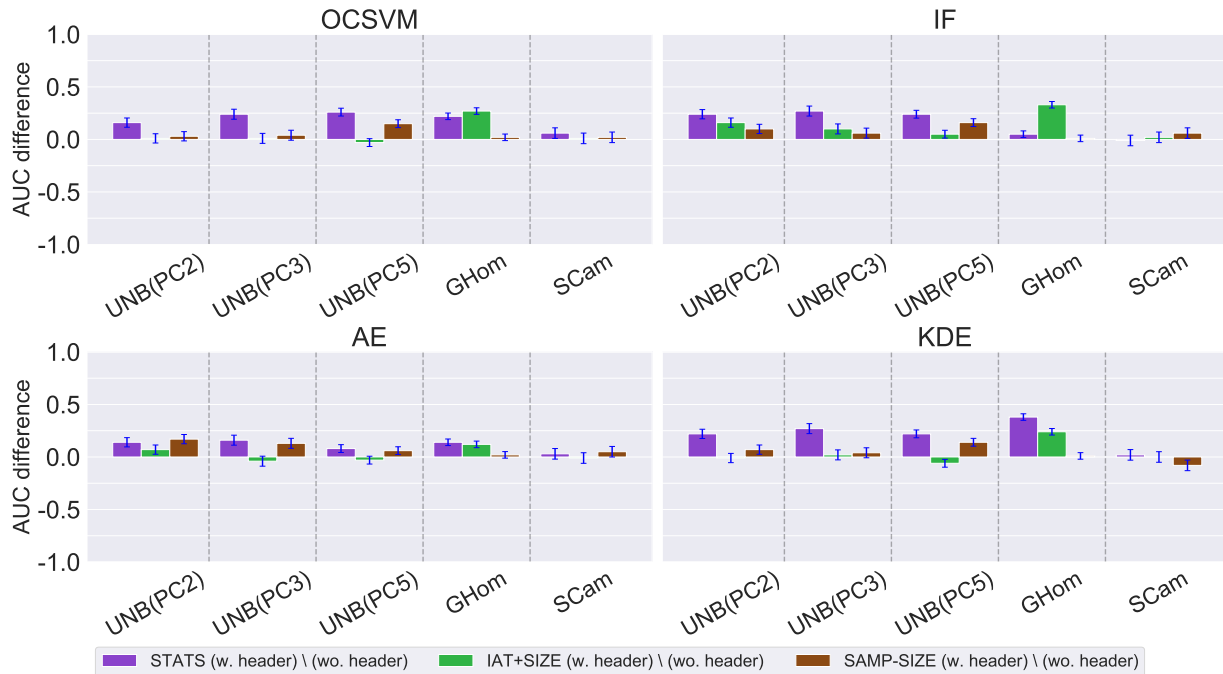


Figure 9: Differences in AUC due to including vs. excluding packet header information with best parameters.



Figure 10: Differences in AUC due to including vs. excluding packet header information generated by GMM and PCA with best parameters.

C Evaluation with Default Parameters

Table 8: AUCs for 4 ML approaches on basic feature representations with default parameters.

Detector	Dataset	STATS	SIZE	IAT	IAT+SIZE	SAMP-NUM	SAMP-SIZE
OCSVM	UNB(PC1)	0.56	0.20	0.40	0.89	0.66	0.74
	UNB(PC2)	0.43	0.66	0.82	0.74	0.79	0.85
	UNB(PC3)	0.30	0.83	0.82	0.85	0.82	0.85
	UNB(PC4)	0.42	0.58	0.82	0.76	0.67	0.78
	UNB(PC5)	0.41	0.64	0.84	0.82	0.75	0.74
	CTU	0.96	0.97	0.95	0.96	0.88	0.88
	MAWI	0.43	0.38	0.56	0.38	0.58	0.59
	TV&PC	1.00	1.00	0.94	0.98	0.70	0.86
	GHom	0.73	0.97	0.10	0.11	0.95	0.94
	SCam	0.58	0.51	0.54	0.61	0.59	0.58
	SFrig	0.91	0.90	0.77	0.84	0.94	0.95
	BSTch	0.96	0.98	0.94	0.98	0.92	0.92
	IF	UNB(PC1)	0.47	0.45	0.48	0.69	0.65
UNB(PC2)		0.65	0.61	0.68	0.74	0.80	0.75
UNB(PC3)		0.61	0.62	0.70	0.73	0.80	0.72
UNB(PC4)		0.45	0.46	0.61	0.61	0.81	0.70
UNB(PC5)		0.47	0.59	0.69	0.70	0.78	0.72
CTU		0.94	0.92	0.78	0.88	0.83	0.84
MAWI		0.86	0.68	0.53	0.66	0.56	0.55
TV&PC		0.95	0.98	0.89	0.99	0.73	0.78
GHom		0.86	0.68	0.44	0.47	0.96	0.96
SCam		0.51	0.51	0.52	0.54	0.56	0.56
SFrig		0.96	0.95	0.54	0.94	0.93	0.93
BSTch		0.94	0.98	0.94	0.98	0.96	0.96
AE		UNB(PC1)	0.66	0.39	0.33	0.75	0.78
	UNB(PC2)	0.74	0.54	0.56	0.81	0.78	0.76
	UNB(PC3)	0.65	0.56	0.71	0.81	0.83	0.78
	UNB(PC4)	0.60	0.39	0.63	0.74	0.85	0.86
	UNB(PC5)	0.79	0.25	0.37	0.79	0.84	0.85
	CTU	0.91	0.95	0.80	0.96	0.80	0.76
	MAWI	0.45	0.50	0.48	0.60	0.57	0.54
	TV&PC	1.00	1.00	0.96	0.99	0.77	0.88
	GHom	0.77	0.62	0.33	0.70	0.96	0.95
	SCam	0.61	0.61	0.56	0.61	0.59	0.55
	SFrig	0.92	0.78	0.71	0.91	0.96	0.96
	BSTch	0.95	0.87	0.97	0.98	0.96	0.95
	KDE	UNB(PC1)	0.28	0.37	0.51	0.92	0.74
UNB(PC2)		0.59	0.63	0.82	0.74	0.77	0.80
UNB(PC3)		0.52	0.78	0.82	0.83	0.82	0.84
UNB(PC4)		0.37	0.51	0.71	0.77	0.81	0.84
UNB(PC5)		0.33	0.62	0.84	0.84	0.74	0.81
CTU		0.96	0.94	0.93	0.97	0.82	0.84
MAWI		0.66	0.38	0.56	0.41	0.57	0.56
TV&PC		1.00	1.00	0.95	0.98	0.66	0.83
GHom		0.55	0.94	0.05	0.46	0.96	0.95
SCam		0.49	0.51	0.55	0.60	0.56	0.57
SFrig		0.94	0.91	0.73	0.77	0.94	0.94
BSTch		0.96	0.96	0.95	0.98	0.92	0.91

Table 9: AUCs for 2 additional ML approaches (GMM and PCA) on basic feature representations with default parameters.

Detector	Dataset	STATS	SIZE	IAT	IAT+SIZE	SAMP-NUM	SAMP-SIZE
GMM	UNB(PC1)	0.37	0.23	0.16	0.81	0.76	0.73
	UNB(PC2)	0.56	0.52	0.65	0.71	0.85	0.54
	UNB(PC3)	0.52	0.61	0.75	0.90	0.81	0.56
	UNB(PC4)	0.40	0.47	0.60	0.57	0.81	0.82
	UNB(PC5)	0.36	0.43	0.70	0.71	0.71	0.73
	CTU	0.95	0.92	0.89	0.84	0.88	0.84
	MAWI	0.65	0.37	0.52	0.40	0.60	0.58
	TV&PC	1.00	0.88	0.86	0.57	0.60	0.80
	GHom	0.33	0.30	0.06	0.39	0.96	0.96
	SCam	0.47	0.46	0.52	0.60	0.54	0.59
	SFrig	0.73	0.91	0.82	0.93	0.96	0.95
	BSTch	0.96	0.95	0.93	0.99	0.93	0.90
	PCA	UNB(PC1)	0.66	0.29	0.27	0.65	0.72
UNB(PC2)		0.59	0.67	0.43	0.32	0.84	0.77
UNB(PC3)		0.71	0.48	0.70	0.48	0.73	0.68
UNB(PC4)		0.65	0.22	0.64	0.63	0.89	0.69
UNB(PC5)		0.73	0.29	0.44	0.78	0.66	0.67
CTU		0.95	0.94	0.80	0.97	0.77	0.79
MAWI		0.65	0.71	0.46	0.54	0.59	0.51
TV&PC		0.98	0.97	0.40	0.99	0.94	0.94
GHom		0.20	0.71	0.30	0.97	0.96	0.95
SCam		0.55	0.61	0.49	0.64	0.62	0.58
SFrig		0.96	0.90	0.76	0.97	0.96	0.95
BSTch		0.95	0.98	0.97	0.98	0.97	0.96

C.1 Effect of Fourier Domain Representation

The figures below show differences in model accuracy for Fourier domain representation vs. raw timeseries representations for different models and datasets. Fourier domain representations in general do not improve model accuracy.

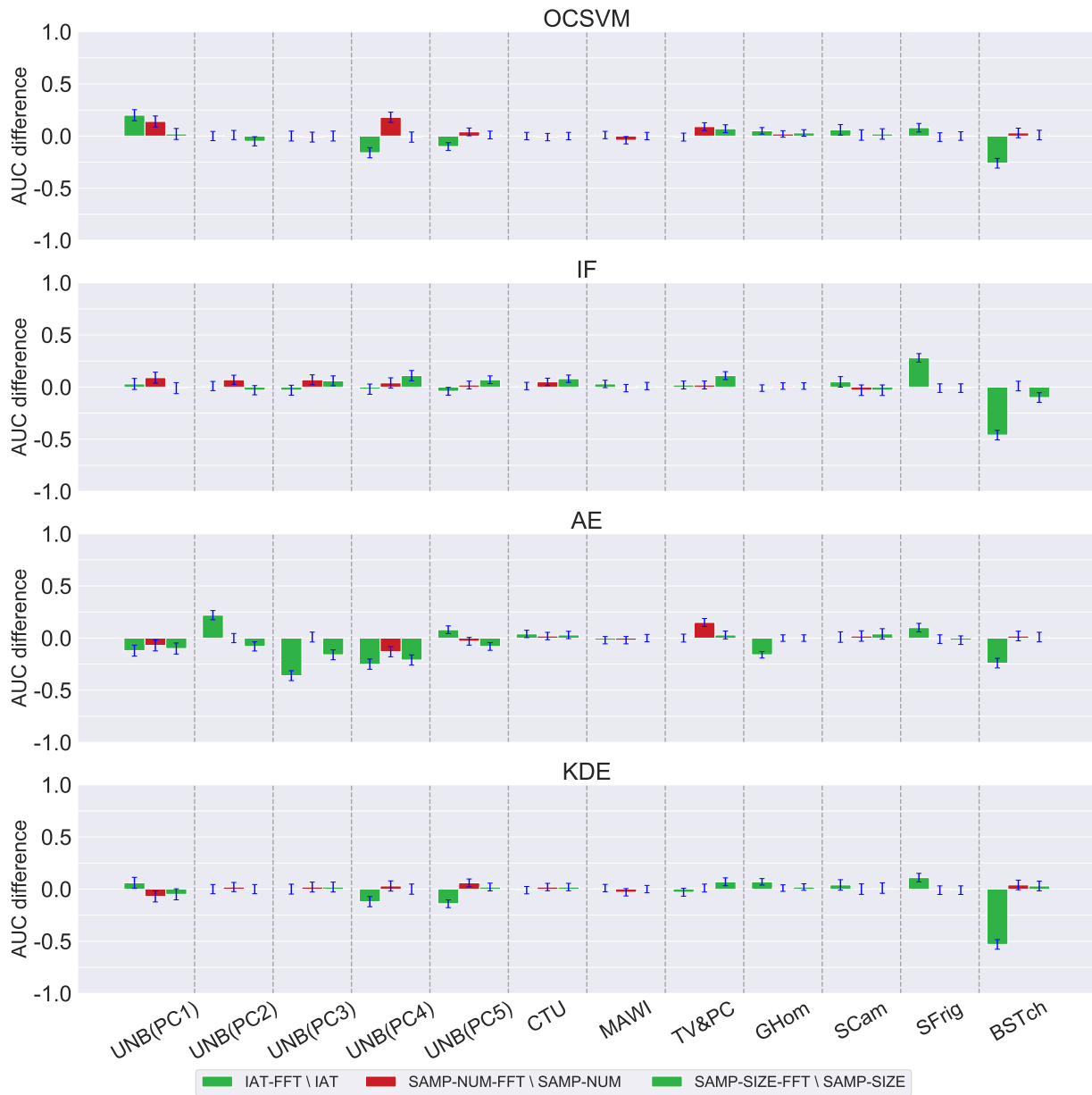


Figure 11: Difference in AUC for FFT vs. raw time series representations with default parameters.

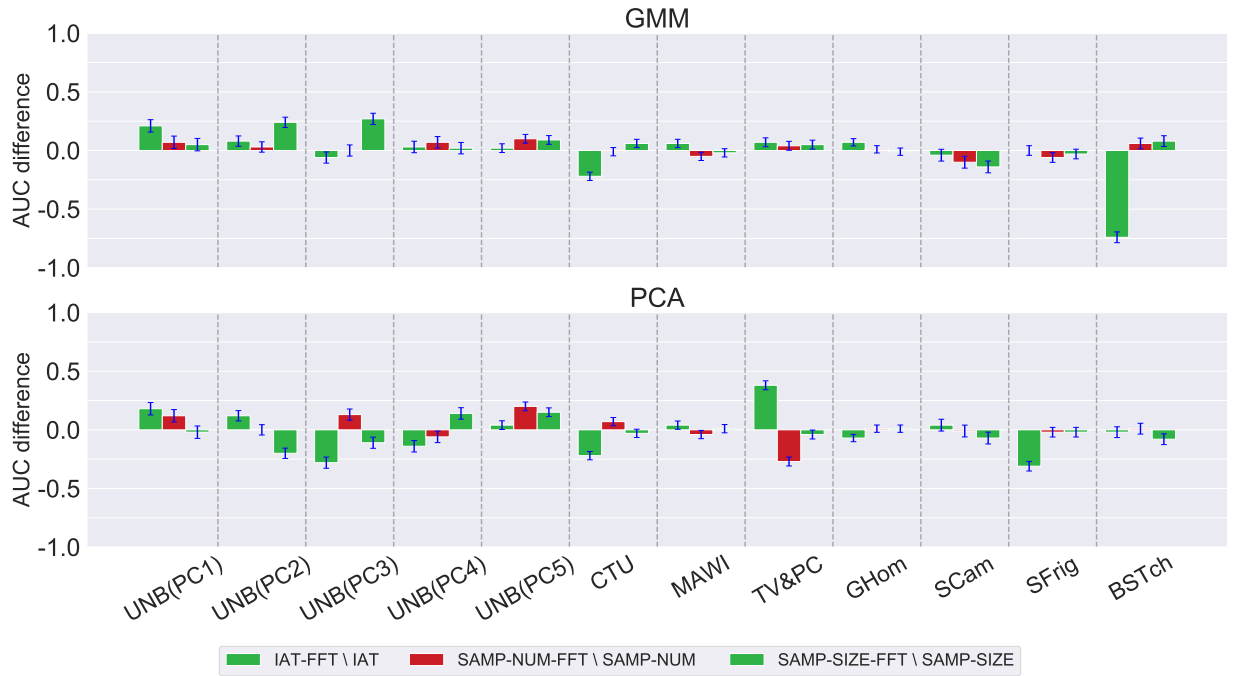


Figure 12: Difference in AUC for FFT vs. raw time series representations generated by GMM and PCA with default parameters.

C.2 Effect of Packet Size Information

The figures below show differences in model accuracy as a result of including packet size information for different models and datasets. Packet size information generally improves model accuracy.

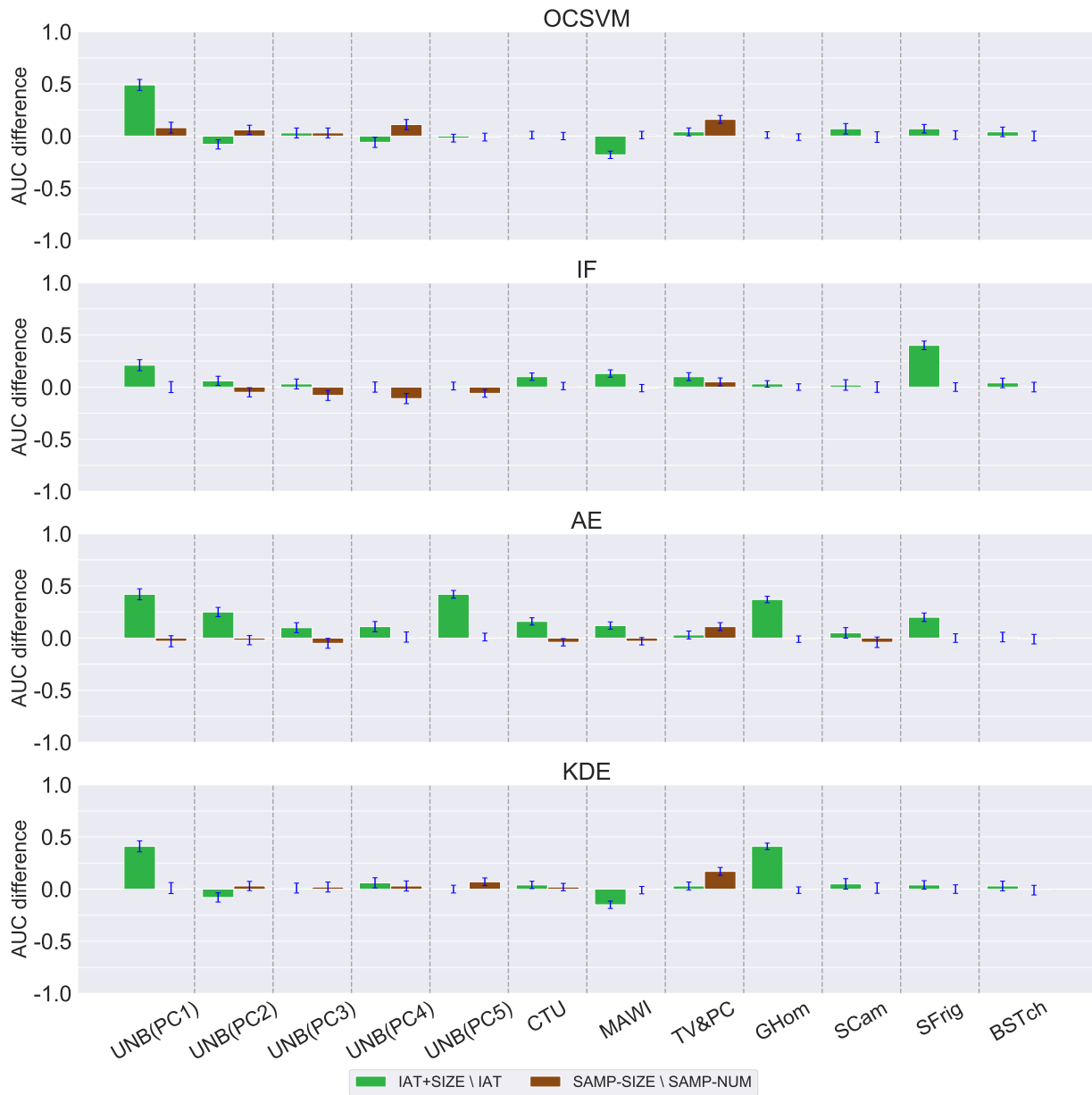


Figure 13: Differences in AUC due to including vs. excluding packet size information with default parameters.

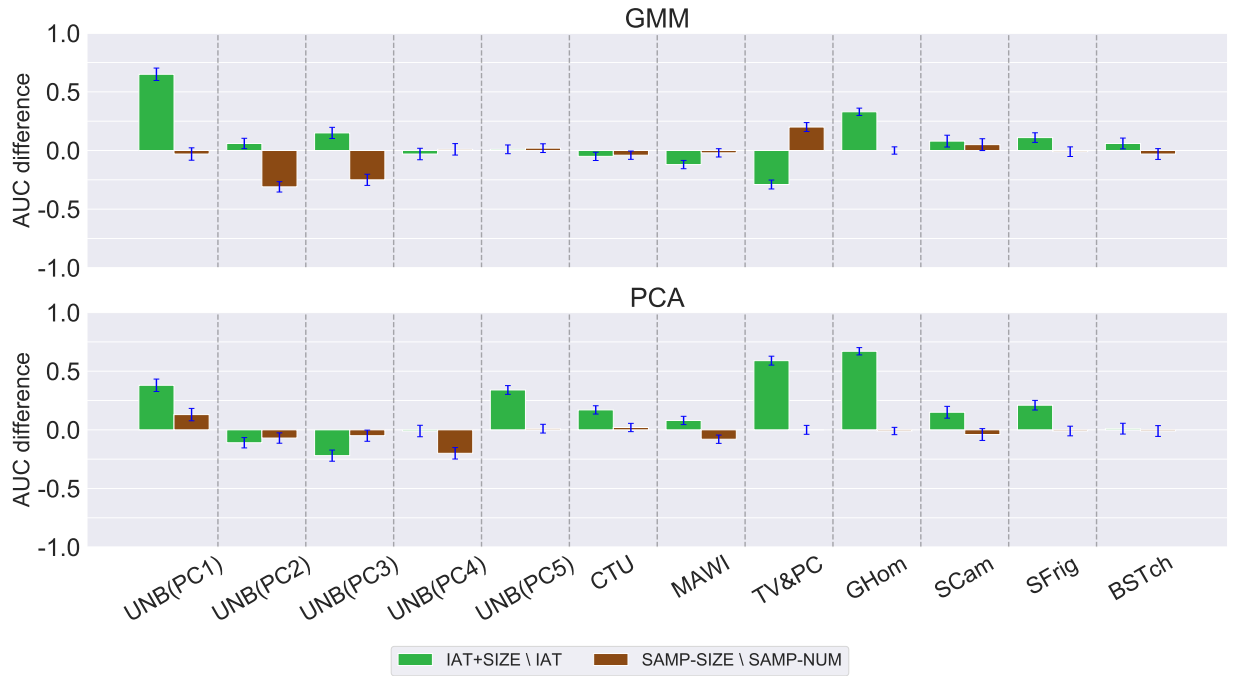


Figure 14: Differences in AUC due to including vs. excluding packet size information generated by GMM and PCA with default parameters.

C.3 Effect of Packet Header

The figures below show differences in model accuracy as a result of including packet header information for different models and datasets. Packet header information generally improves model accuracy.

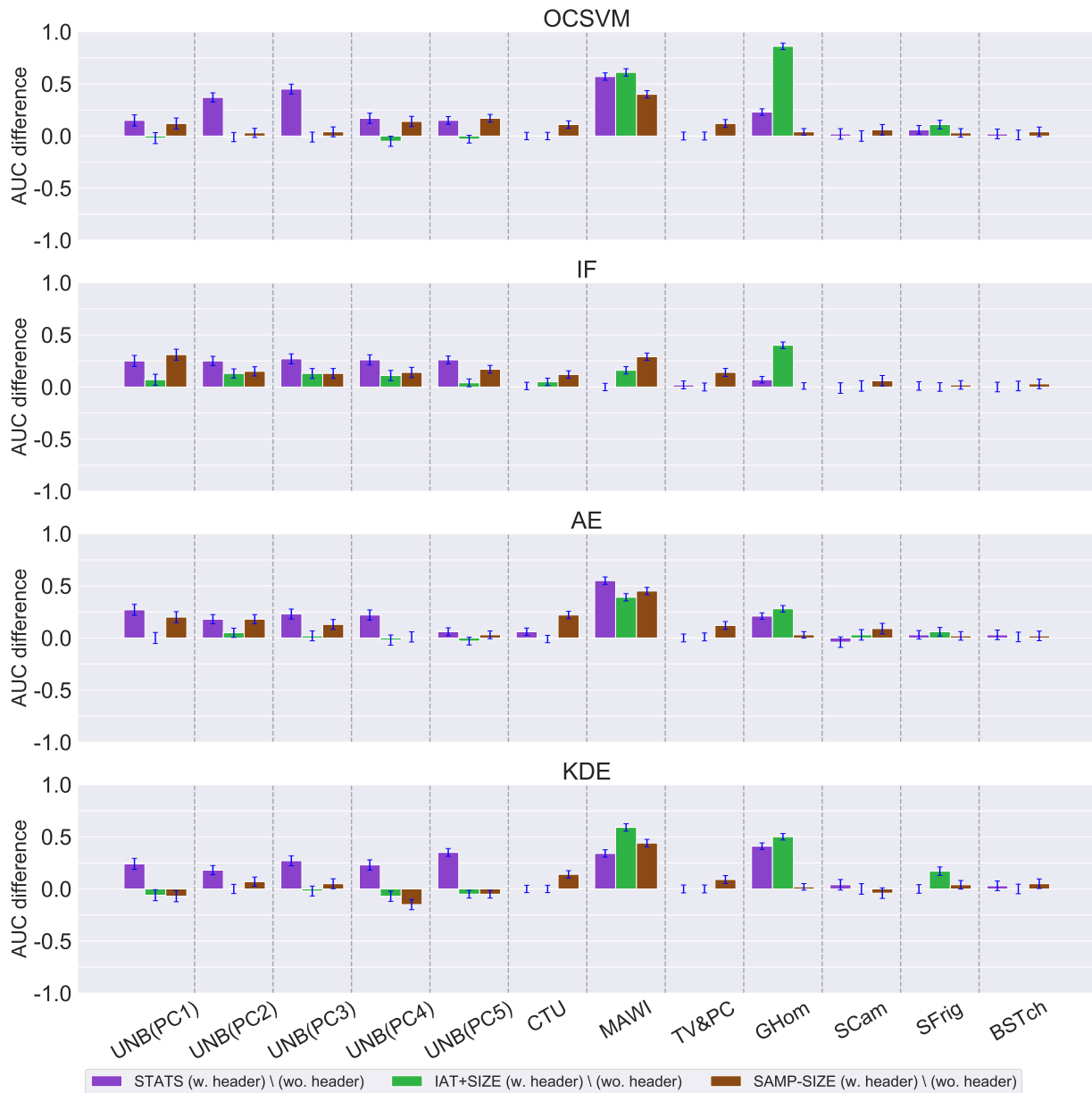


Figure 15: Differences in AUC due to including vs. excluding packet header information with default parameters.

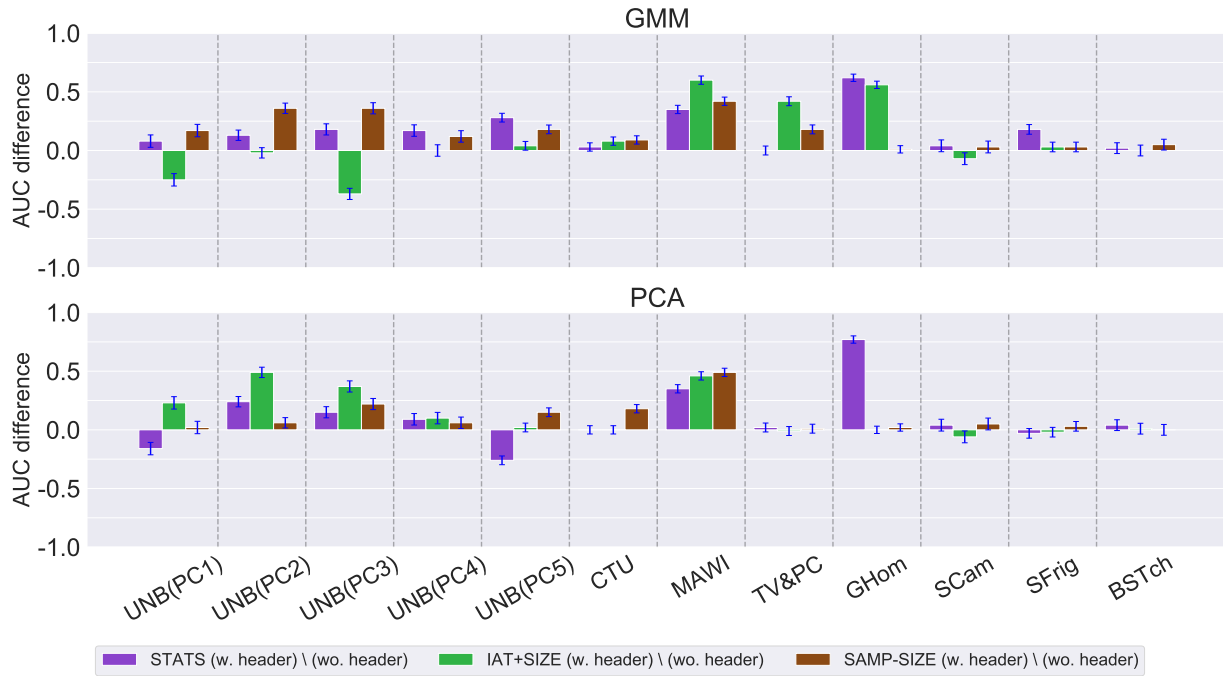


Figure 16: Differences in AUC due to including vs. excluding packet header information generated by GMM and PCA with default parameters.